This is a repository copy of *Some experiments on the microindentation of digital audio tape*.

Article:

Some Experiments on the Micro-Indentation of Digital Audio Tape

R. S. Dwyer-Joyce[*], Y. Ushijima[#], Y. Murakami[#], and R. Shibuta[†]

[*]   Department of Mechanical Engineering, University of Sheffield, Mappin Street, Sheffield S1 3JD.

[#]   Department of Mechanical Science and Engineering, Kyushu University, Hakozaki 6-10-1, Higashi-ku, Fukuoka, Japan.

[†]   Mitsubishi Chemical Corporation. Yokohama Research Centre, Yokohama

Abstract

The durability of digital audio tape is a function of the elastic and plastic properties of the magnetic layer and substrate. In this work a micro-indentation method has been used to estimate these properties. The loading part of the compliance curve (load against indentor penetration) is analysed to obtain magnetic layer hardness. The unloading part is used to determine the reduced elastic modulus. Indentations at various depths have been recorded and an extrapolation technique used to predict layer properties. Rate dependence of the magnetic layer has been studied through constant loading rate tests. Results are presented isochronally, to indicate any viscous elastic-plastic non-linearities.

Nomenclature

h depth of indentor penetration (measured with the undeformed surfaces as a datum)

h_f final recorded depth of penetration (depth of residual indentation)

h_c contact depth (vertical distance from the edge of the contact area to the indentor tip)

h_{max} maximum penetration of the indentor

P load applied to indentor

P_{max} maximum load applied to indentor

A_c projected area of contact under load

E^* reduced modulus

S contact stiffness, dP/dh

Introduction

Digital audio tape (DAT) consists of a polymer strip coated with a thin layer of magnetic particles suspended in a polymeric binder. A polyurethane backcoat is also sometimes applied. Figure 1 shows a section through the tape used in these experiments. The substrate is 9 µm thick polyethylene tetraphthalate (PET) and the magnetic layer is a 2 µm thick suspension of iron oxide particles in a binder.

The durability of magnetic tape is a function of both the properties of the magnetic coating and the substrate. For optimum wear resistance a hard, low modulus layer may be desirable. To minimise layer/substrate interfacial shear stress it is important to match the elastic properties of the two materials. In addition, when modelling the behaviour of this tape in normal operation it is important to know its elastic and plastic properties.

Figure 1. Section through the magnetic tape used in this study.

Tape substrate elastic properties may be measured in a microtensile test. However measurement of layer properties is more difficult. Recently the availability of micro and nano indentation testers has made these measurements possible. In principle, a diamond indentor (commonly a triangular base Berkovitch type) is pressed onto the specimen surface held for a pre-set time and then released. Throughout the loading cycle the applied load and depth of penetration are sensed by inductive transducers.

Analysis of Load Penetration Depth Indentation Curves

A typical load penetration depth curve is shown in Figure 2. During indentor loading, the material undergoes both elastic and plastic deformation. This loading part of the curve, with the subtraction of the elastic deformation, is used to determine the hardness of the material. The unloading part of the curve is essentially elastic and with some analysis gives information about the elastic material properties. The behaviour of the material during a load hold or under various loading rates can be used to determine rate dependent properties.
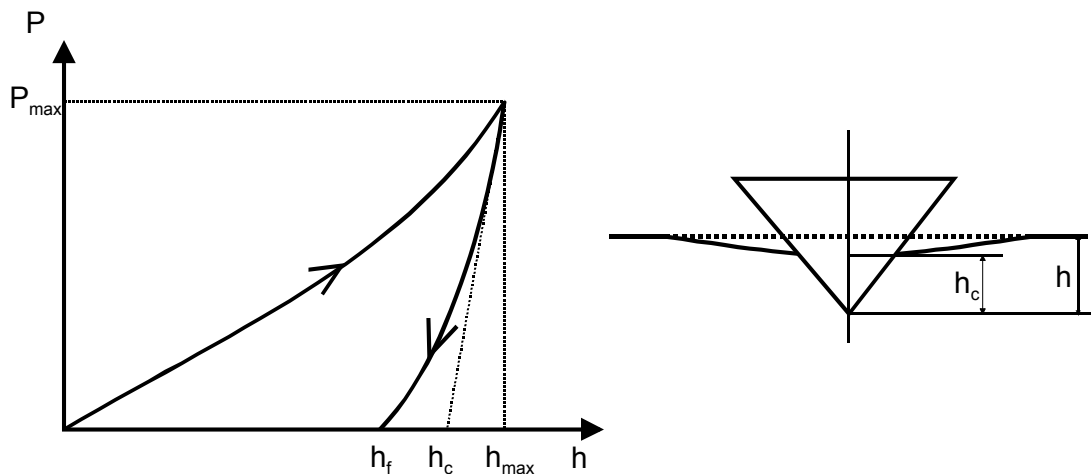
Figure 2. Schematic diagram of a typical load/penetration micro-indentation curve.

Interpretation of the Loading Curve - Material Hardness

The hardness H, is defined as the mean pressure under the indentor:

$$H = \frac{P_{\max}}{A_c} \tag{1}$$

where P_{max} is the applied load and A_c is the projected area of the impression under load.

In a conventional Vickers hardness test the area of the residual impression is measured optically and used in place of the area of the impression under load. Stilwell & Tabor (1) showed that this is acceptable since when a indentation is unloaded there is little elastic recovery of the impression sides (although the depth recovers substantially).

A depth sensing hardness tester records only the total penetration, h. Pethica (2) demonstrated that using the penetration depth and the shape function of the indentor to calculate, A_c the

contact area gives only an approximate value of the hardness. This is because the penetration depth incorporates both the contact depth and the elastic deformation of the surrounding hinterland (as shown in figure 2). Clearly only the depth in contact should be used in the determination of A_c and hence the hardness.

Doerner and Nix (3) showed that for some materials the first part of the unloading curve is linear. This implies that within this region, the contact area remains constant (i.e. flat punch behaviour $P \propto h$). Extrapolating this straight line part of the curve gives the contact depth h_c under the maximum load P_{max}. (as shown in figure 2).

Oliver and Pharr (4) showed that for many materials a linear initial unloading does not occur. They suggest a power law fit, $P \propto (h-h_c)^m$ to the unloading curve is a more general behaviour. Then the slope of the fit at the maximum load gives the contact depth.

Alternatively one may estimate a relationship between the total penetration and the contact depth by assuming an ideal shape for the indentor, using the relations of Sneddon (5). Then h_c/h is given by $2/\pi$, $1/2$, or $5/8$ for a cone, circular punch, or parabolic profile indentor respectively.

Briscoe and Sebastian (6) also curve fit to the unloading data using a form $P \propto E^*(h-h_0)^m$. However they introduce a zero correction to accommodate the difficulties micro-indentation devices have in sensing the specimen surface.

Once the contact depth has been determined the contact area is readily obtained from the geometry of the diamond pyramid (which is assumed to remain undeformed). For a perfect Berkovitch indentor:

$$A_c = 24.56 h_c^2 \tag{2}$$

Real indentor diamonds will deviate from this perfect geometry. Indentations at low penetrations are particularly susceptible to tip imperfection. Calibration of the tip geometry may be carried out to determine this area function to greater accuracy (3,4,6).

Interpretation of the Unloading Curve - Elastic Properties

Stilwell and Tabor (1) showed that the unloading of a conical indentor was essentially an elastic process. As such , it can be considered as the elastic loading of a cone into a conical cup. The analysis for an axisymmetric cone, presented by Love (7), gives a relationship between the load and penetration:

$$\frac{P}{E^*} = \frac{2}{\pi} \tan\alpha \, h^2 \tag{3}$$

Where α is the apical semi-angle of the cone and E^* is the reduced modulus:

$$\frac{1}{E^*} = \frac{1-v_s^2}{E_s} + \frac{1-v_i^2}{E_i} \tag{4}$$

where, E and v are the Young's modulus and Poisson's ratio of the materials and s and i signify the specimen and the indentor respectively.

Analytical solutions for the Berkovitch type indentor are not available. Murakami et al (8) carried out a finite element analysis of a Berkovitch indentor and showed:

$$\frac{P}{E^*} = 1.70 \frac{2}{\pi} \alpha \, h^2 \tag{5}$$

Where α is the included face angle of the Berkovitch indentor (α = 65.3º). Larsson et al (9) found a similar relation by the same method:

$$\frac{P}{E*} = 2.189 \, (1 - 0.21\nu - 0.01\nu^2 - 0.41\nu^3) \, h^2 \tag{6}$$

Both these relationships assume the residual impression has no effect on the unloading. This is generally not the case. The form of the unloading curve is dependent on the size of the residual impression.

An alternative method for determining the modulus was first given by Doerner and Nix (3) using the relations of Sneddon (5). The stiffness of the contact at the point of unloading for any solid of revolution is given by:

$$S = \frac{dP}{dh} = \frac{2}{\sqrt{\pi}} \, E^* \sqrt{A_c} \tag{7}$$

Using the initially linear part of the unloading curve, both the stiffness and the contact depth are determined and hence the reduced modulus calculated. Oliver and Pharr (4) obtain this stiffness by differentiating the power law fit (as described above) to perform a similar calculation. Both methods are reported to give close agreement with conventional testing methods for a wide range of materials. It is this last method which has been used to determine elastic reduced modulus in this study.

Indentation Experiments

Tape samples (with and without the magnetic layer) were mounted on glass slides and a series of micro-indentation experiments carried out at a range of loads and loading rates. The indentation device and tape specimen are maintained at a constant temperature and humidity throughout the test. Initial tests were performed at the highest loading rate to determine instantaneous response of the material. Subsequent tests were performed with hold periods (at constant load) and at slower rates.

High Loading Rate Tests

Figure 3 shows a series of load penetration plots recorded at different maximum loads. Figure 4 shows SEM images of the residual impressions.
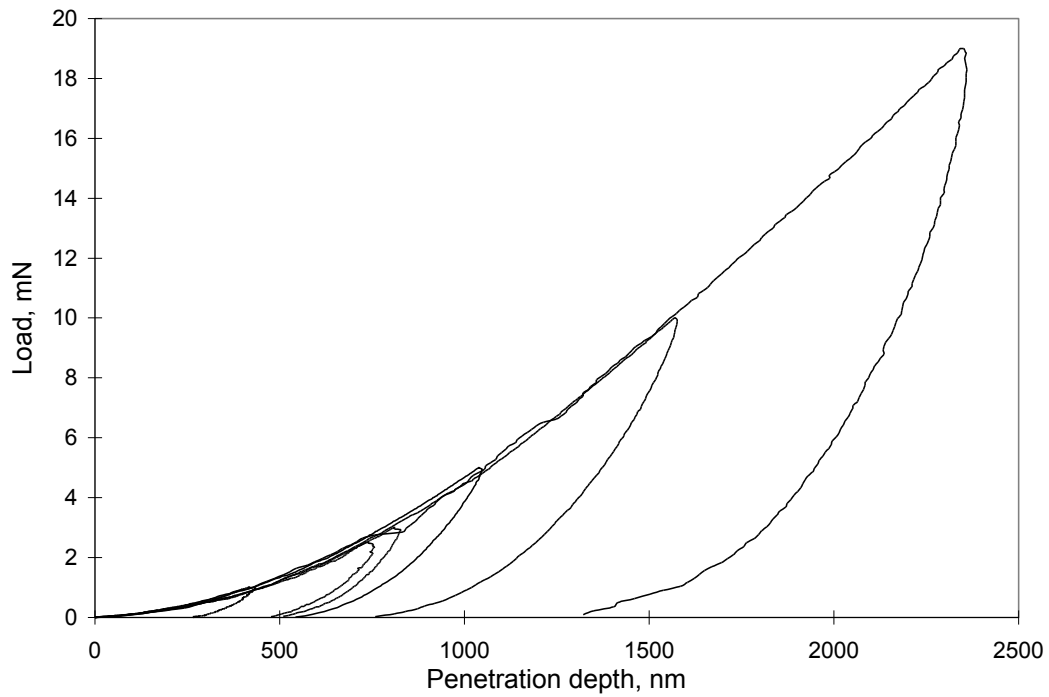
Figure 3. A series of load penetration plots for magnetic tape. Measurement made at high loading rate (0.142 mN/s).

Figure 4. SEM images of residual impressions following Berkovitch micro-indentations.

The modulus has been determined from these unloading curves (using the method of Oliver and Pharr). Figure 5 shows this data plotted against the maximum depth of penetration during the test.
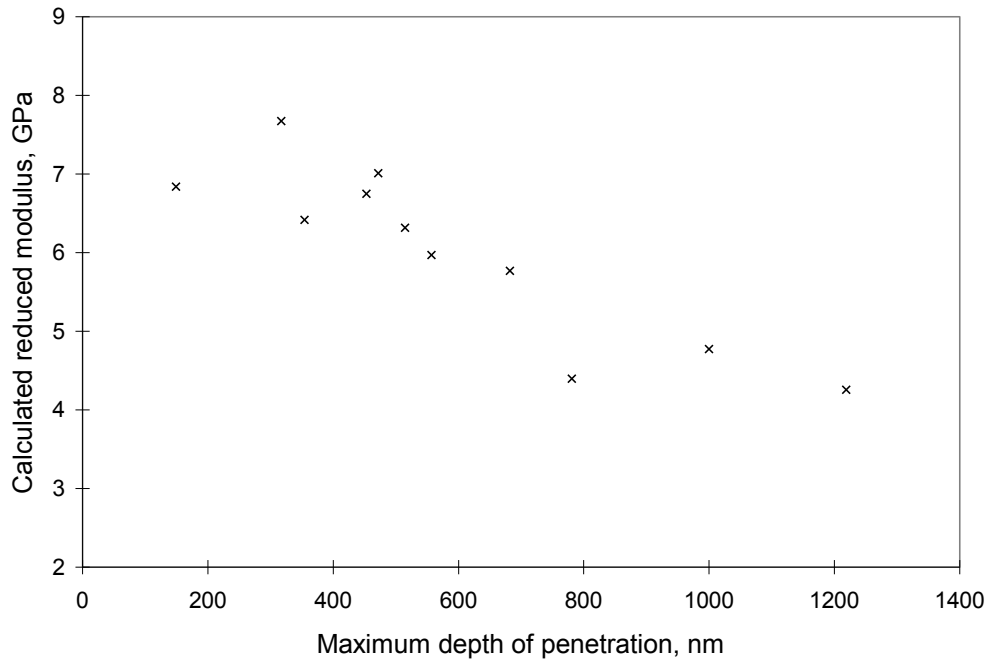
Figure 5. The reduced modulus calculated from a series of indentations on magnetic tape.

At deep penetrations the indentation of the tape is dominated by the properties of the substrate. As the depth of penetration is reduced the properties of the film become more important. It is usual to ensure that when performing indentations on a surface layer, the depth of the penetration should be no more than 10% of the layer thickness. For this relatively soft material this requires loading to less than 1 mN. At low loads the data is subject to scatter caused by surface roughness, tip geometry, and extraneous noise. To improve accuracy we extrapolate the curve in Figure 5 and estimate the layer reduced modulus to be between 7 and 8 GPa.

The hardness of the magnetic layer, as defined by equation 1, has also been determined (again after the method of Oliver and Pharr). Figure 6 shows this hardness as a function of the depth of penetration; a layer hardness of 400 - 450 MPa is predicted. However, a large amount of scatter is apparent, probably caused by the anisotropy of the material.
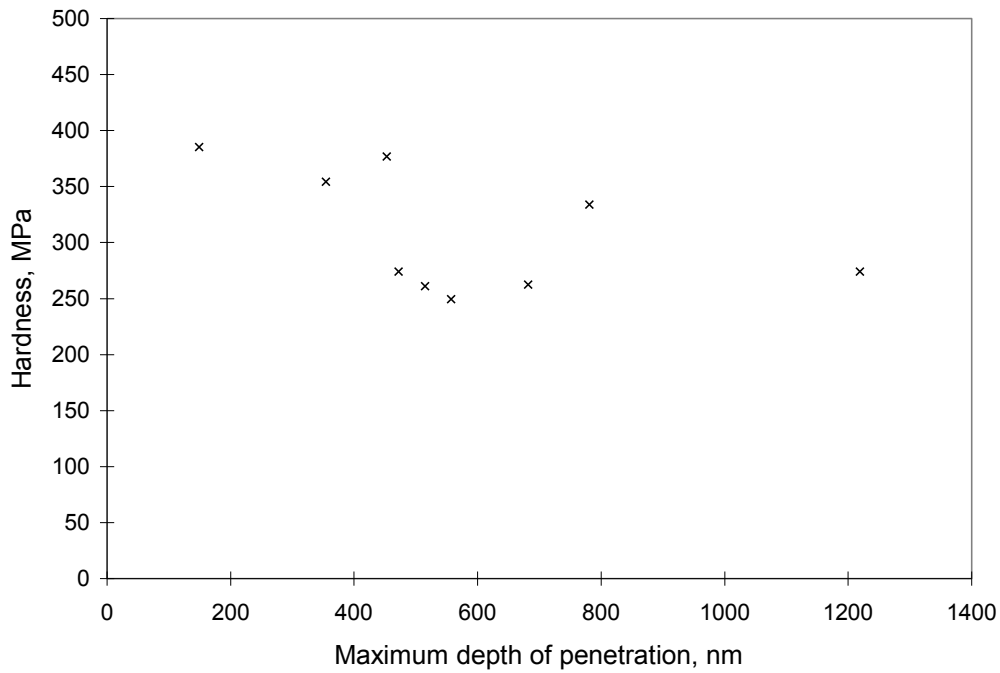
Figure 6. The hardness calculated from a series of indentations on magnetic tape.

Load Hold Tests

At maximum depth we hold the load constant for a pre-set period of time. Creep effects are manifested as an increase in penetration under this fixed load. Figure 7 shows two such tests where the hold times are 1 second and 30 seconds.
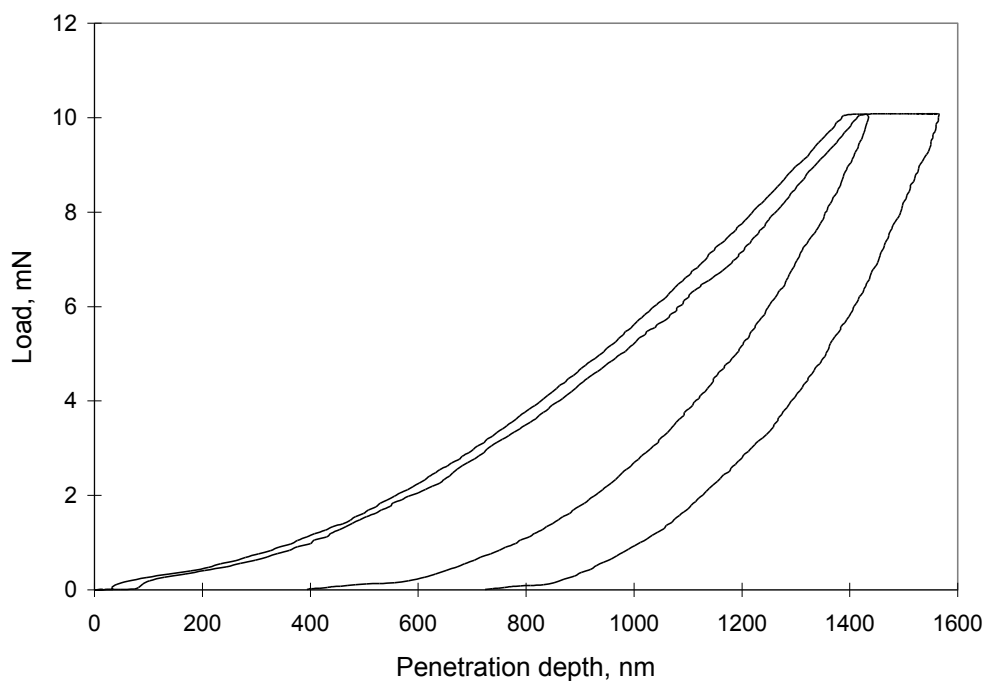

Figure 7. Two constant load hold tests on magnetic tape.

Figure 8 replots the 30 second hold data showing the increase in penetration with time. Some results for brass (normally not subject to creep at room temperature) are also shown to

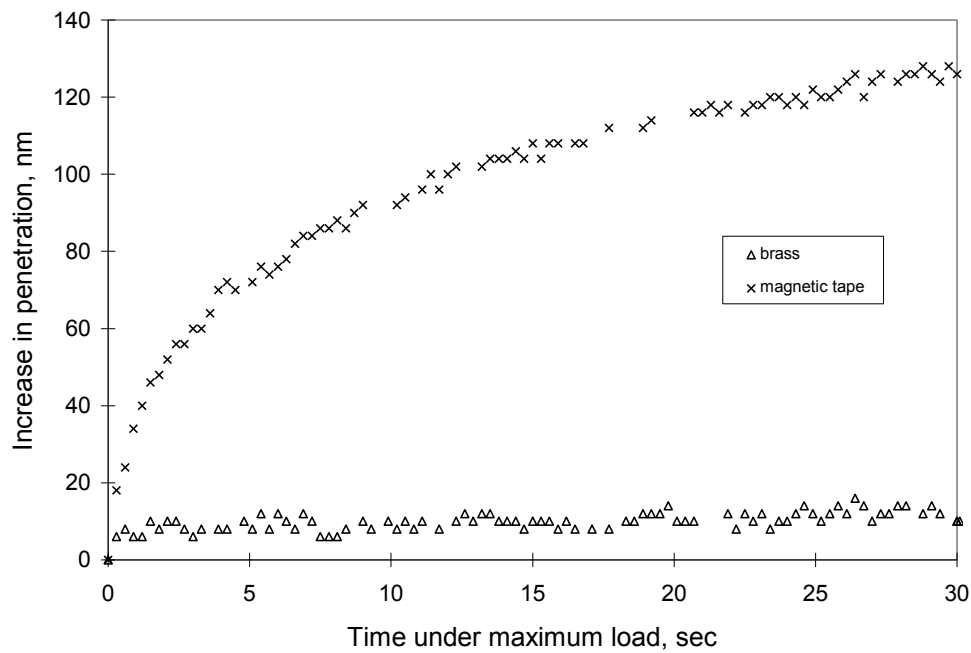demonstrate the stability of the apparatus (measurements like these are susceptible to thermal drift).

Figure 8. Increase in penetration during the hold part of a constant load hold test for both magnetic tape and brass.

The magnetic layer material is clearly creeping under the applied load. Within a few seconds the bulk of the relaxation has occurred. However after this period, some steady state viscous flow is apparent.

During the hold period, although the load is constant, the stress beneath the indentor is reducing as the indentation relaxes. In this test therefore both the stress and strain are varying (over the range $100<\sigma<400$ MPa, $10^{-3} <\dot{\varepsilon}< 10^{1}$ sec) continually.

Maxwell-Voigt and other types of visco-elastic/plastic deformation models become more difficult to implement under these conditions. Ion et al (10) give a detailed study of these flow properties for drawn and amorphous PET. In this study, given the complex geometrical non-linearities, we choose to investigate rate dependence of the *P* vs *h* compliance behaviour rather than the stress strain behaviour. We do this by the analysis of a series of constant loading rate tests.

Constant Loading Rate Tests

Figure 9 shows a series of indentation tests carried out at a range of constant loading rates. Clearly, when loading occurs at a lower rate, the depth of penetration is greater. The unloading curves are slightly different; creep is also occurring during the unloading.
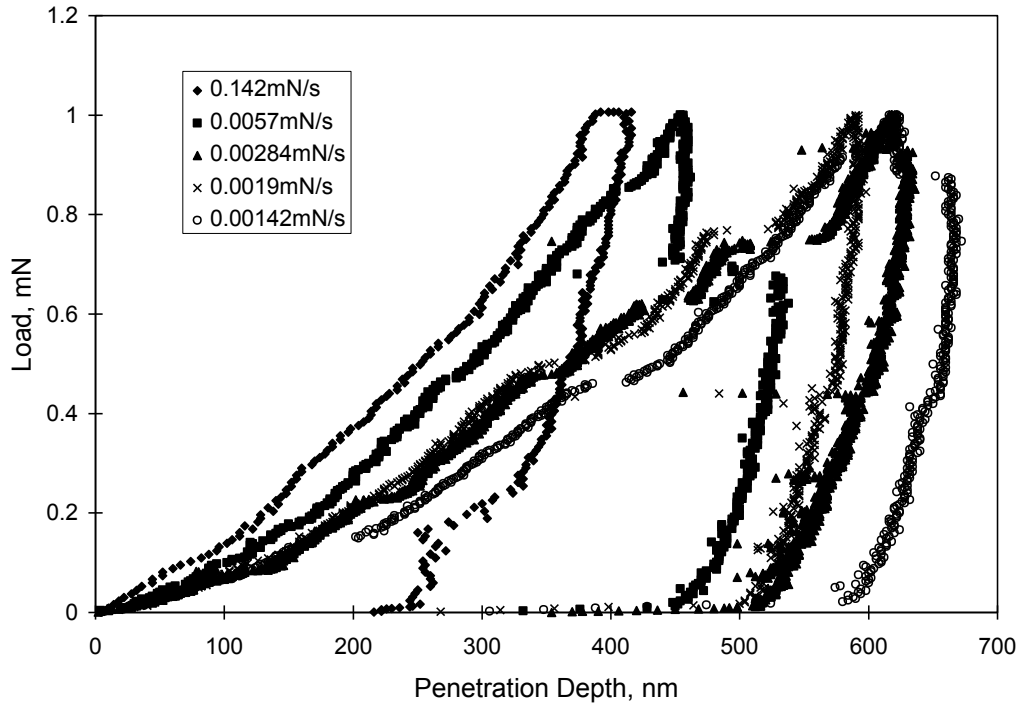
Figure 9. A series of micro-indentation tests on the magnetic layer carried out at a range of loading rates.

If the layer deforms in a linear visco-elastic or plastic manner when subjected to a constant stress, σ then the strain, ε, after a period of time, t is given by;

$$\varepsilon(t) = J(t)\sigma \qquad (8)$$

where J is a creep compliance function (and is independent of stress). Plotting stress and strain data at constant time (isochrones) gives a series of straight line stress strain lines where the slope depends on the time period. Any non-linear polymer deformation behaviour would be indicated by deviation from the straight line.

We follow a similar analysis here. The loading data from Figure 9 is replotted as isochrones in Figure 10. There is a scarcity of data, since the number points is the same as the number of loading rate tests performed.
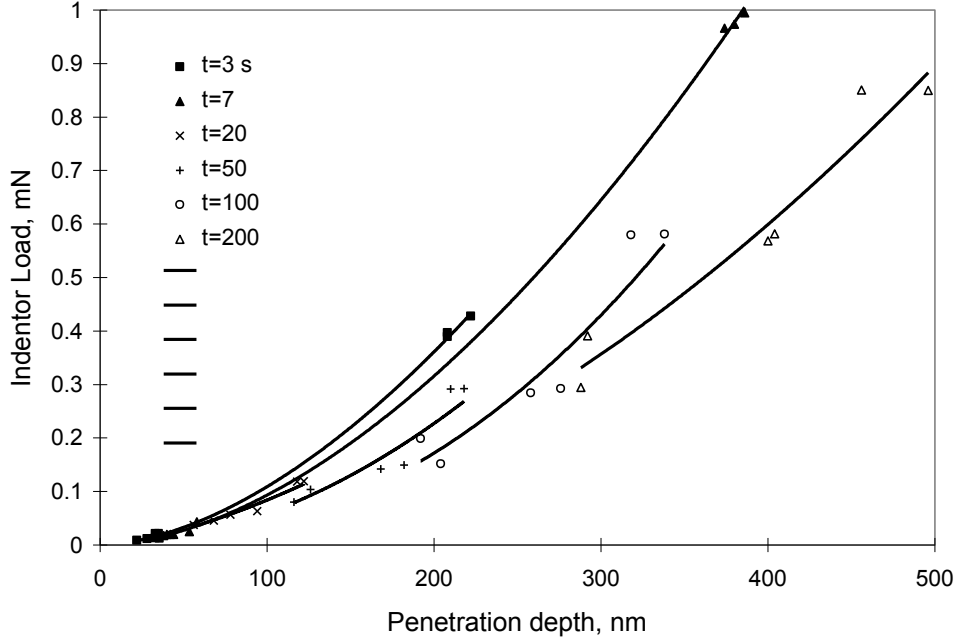
Figure 10. The loading part of a series of constant loading rate micro-indentations on magnetic layer materials. Data plotted at constant time (isochrones).

Typically power law curves of the form $P=kh^n$ may be fitted to loading data. The constant k is a function of the material stiffness (for both the elastic and plastic deformation) and the geometry of the indentor. If the polymer is linear visco-elastic/plastic, then we would expect a series of curves where the stiffness k varies with time but the exponent n remains constant.

Curve fitting to the data, shows that within the experimental scatter, this is the case; the exponent n varies between 1.6 - 1.9 with no apparent trend. No gross non-linearities are observed over this stress/strain rate range.

Discussion

In this work we have determined the reduced modulus of the magnetic using a standard indentation technique (Oliver and Pharr). Performing indentations at shallow penetrations has a number of difficulties (shape of the indentor tip, machine compliance, extraneous noise, thermal drift etc.). The extrapolation methods provides a simple method for estimating the layer properties avoiding some of these problems.

The modulus of the substrate material, without the magnetic layer, was also estimated by the indentation method. A reduced modulus of between 3 and 4 GPa was determined. This value agrees qualitatively with measurements on PET by Ion (10) 2.4 - 3 GPa, Bushan (11) 2.7 GPa, and Billmeyer (12) 3.6 - 5.6 GPa. Clearly PET comes in different forms (amorphous or drawn) so only qualitative agreement is expected.

The magnetic layer is a polymer binder with a suspension of iron oxide particles. A rough estimate for the modulus of such a filled polymer may be obtained from the modulii of the constituent components and the volume fraction, V_f:

$$E = \left(\frac{V_f}{E_p} + \frac{1 - V_f}{E_m} \right)^{-1} \tag{9}$$

where the subscripts p and m indicate the particle and matrix material. Performing this calculation for the magnetic tape layer (using appropriate values for the volume fraction and

10

component modulii) predicts a modulus 6 - 8 GPa. This estimate is consistent with that measured by micro-indentation.

The magnetic layer is anisotropic; both the tape microstructure and the particles are aligned parallel to the surface. The indentation method will determine a modulus more closely linked to a direction normal to the surface (since the majority of the strains during indentation are in the normal direction). In tribological studies of surface damage and wear it is not unreasonable to use this modulus (i.e. as a resistance to penetration) but if it is bending or flexure of the tape which is of interest then it may not be wholly appropriate.

The indentation method determines the reduced modulus (defined in equation 4). The modulus of the diamond indentor material is large compared with the polymer and so may be neglected. Clearly the reduced modulus incorporates Poisson's ratio of the layer material. At present it is not possible to separate Poisson's ratio and Young's modulus by an indentation technique. This is a serious limitation which may only be overcome by assuming a value for Poisson's ratio for the film material.

This isochronal analysis of the compliance curves (figure 10) provides a simple method for displaying rate dependent properties. It overcomes the complexities of the stress/strain state during indentation. It is difficult to extract hardness and modulus from such data since both viscous elastic and plastic deformation occur during both loading and unloading. It is still difficult to fully classify the nature of the creep process but the isochronal method indicates that there are no major non-linearities. This type of presentation is useful for the engineer. If the tribological process (e.g. tape/head contact or tape/roller contact) occurs over some particular duration we can use the isochrone appropriate at that duration to give load deflection response.

Conclusions

1. A micro-indentation method has been used to measure the properties of the magnetic layer on digital audio tapes. A series of indentations are recorded at reducing ultimate loads and an extrapolation technique used to predict layer properties (i.e. when the effect of the substrate on indentation is negligible).

2. The hardness is deduced from the loading part of the curve (by subtracting the elastic deformation of the impression hinterland). For the layer $H = 400\text{-}450$ MPa.

3. The reduced modulus is deduced from the unloading part of the curve (by determining the stiffness at the point of unloading). For the layer $E^* = 7\text{-}8$ GPa and for the substrate $E^* = 3\text{-}4$ GPa.

4. Isochronal plotting of the P vs. h compliance data is a useful method for displaying rate dependence. Within the stress and strain rates tested no large non-linear behaviour was apparent.

References

1. Stilwell, N.A. and Tabor, D., (1961). 'Elastic Recovery of Conical Indentations', Phys. Proc. Soc., 2, 169-180.

2. Pethica, J. B., Hutchinson, R., and Oliver, W.C., (1983). 'Hardness measurement at penetration depths as small as 20 nm', Philosophical Magazine A, Vol. 48, 593-606.

3. Doerner, M.F. and Nix, W.D., (1986). 'A method for interpreting the data from depth-sensing indentation instruments', J. Mater. Res. 1(4), July/August, 601-609.

4. Oliver, W.C. and Pharr, G.M., (1992). 'An improved technique for determining hardness and elastic modulus using load and displacement sensing indentation experiments', J. Mater. Res., Vol. 7, No. 6, June, 1564-1583.

5.   Sneddon, I.N., (1965). 'The relaxation between load and penetration in the axisymmetric Boussinesq problem for a punch of arbitrary profile', Int. J. Engng Sci., Vol. 3, 47-57.

6.   Briscoe, B.J., Sebastian,K.S., and Sinha, S.K., (1996). 'Application of the compliance method to microhardness measurements of organic polymers', Philosophical Magazine A, Vol. 74, No. 5, 1159-1169.

7.   Love, A.E.H, (1939), 'Boussinesq's Problem for a Rigid Cone', Quarterly Journal of Mathematics, Vol. 10, p161.

8.   Murakami, Y., Tanaka, K., Itokazu, M. and Shimamoto, A., (1963). 'Elastic analysis of triangular pyramid indentation by the finite-element method and its application to nano-indentation measurement of glasses', Philosophical Magazine A, Vol. 69, No. 6, 1131-1153.

9.   Larsson, P.L., Giannakopoulos, A.E., Söderlund, E., Rowcliffe, D.J., and Vestergaard, R., (1995). 'Analysis of Berkovitch Indentation', Int. J. Solids Structures, Vol. 33, No. 2, 221-248.

10.   Ion, R.H., Pollock, H.M., and Roques-Carmes,C., (1990). 'Micron-scale indentation of amorphous and drawn PET surfaces', Journal of Materials Science 25, 1444-1455.

11.   Bharat Bhushan, (1997), 'Tribology and Mechanics of Magnetic Storage Devices', IEEE Publications.

12.   Billmeyer, F.W. (1984), 'Textbook of Polymer Science', New York, Interscience.